



## Assimilation of seasonal chlorophyll and nutrient data into an adjoint three-dimensional ocean carbon cycle model: Sensitivity analysis and ecosystem parameter optimization

Jerry F. Tjiputra,<sup>1</sup> Dierk Polzin,<sup>1</sup> and Arne M. E. Winguth<sup>1</sup>

Received 26 April 2006; revised 18 August 2006; accepted 30 August 2006; published 5 January 2007.

[1] An adjoint method is applied to a three-dimensional global ocean biogeochemical cycle model to optimize the ecosystem parameters on the basis of SeaWiFS surface chlorophyll observation. We showed with identical twin experiments that the model simulated chlorophyll concentration is sensitive to perturbation of phytoplankton and zooplankton exudation, herbivore egestion as fecal pellets, zooplankton grazing, and the assimilation efficiency parameters. The assimilation of SeaWiFS chlorophyll data significantly improved the prediction of chlorophyll concentration, especially in the high-latitude regions. Experiments that considered regional variations of parameters yielded a high seasonal variance of ecosystem parameters in the high latitudes, but a low variance in the tropical regions. These experiments indicate that the adjoint model is, despite the many uncertainties, generally capable to optimize sensitive parameters and carbon fluxes in the euphotic zone. The best fit regional parameters predict a global net primary production of  $36 \text{ Pg C yr}^{-1}$ , which lies within the range suggested by Antoine et al. (1996). Additional constraints of nutrient data from the World Ocean Atlas showed further reduction in the model-data misfit and that assimilation with extensive data sets is necessary.

**Citation:** Tjiputra, J. F., D. Polzin, and A. M. E. Winguth (2007), Assimilation of seasonal chlorophyll and nutrient data into an adjoint three-dimensional ocean carbon cycle model: Sensitivity analysis and ecosystem parameter optimization, *Global Biogeochem. Cycles*, 21, GB1001, doi:10.1029/2006GB002745.

### 1. Introduction

[2] To address the long-term global climate concerns about the rising of the atmospheric  $\text{CO}_2$  concentration, it is essential to understand and quantify the framework of the ocean carbon dynamics by evaluating the contributions of different processes simulated in a carbon cycle model. The complex marine ecosystem processes play an important role in controlling the sources and sinks of the ocean carbon budget in the euphotic layer. One way to estimate the sources and sinks of the carbon budget is to use marine ecosystem models, which, depending on their application, have different levels of complexity [see, e.g., Hofmann and Friedrichs, 2002]. However, all ecosystem models contain parameters (e.g., the remineralization rate of fecal pellets or mortality rate of zooplankton) that are poorly constrained and thus need to be explored with sensitivity studies and observational evidence.

[3] Data assimilation techniques, such as the adjoint method (also called variational data assimilation), have recently been used to efficiently estimate the best fit values for marine ecosystem model parameters [Lawson et al.,

1996; Fennel et al., 2001; Losa et al., 2004; Spitz et al., 2001; Friedrichs, 2002; Schartau et al., 2001]. The adjoint method calculates the gradient of model-data misfit with respect to the control variables and uses the gradient information to vary the parameters toward reduced model-data misfit. Past studies have focused on a box model or a specific region of the world ocean. This study will attempt to apply the adjoint data assimilation technique to optimize the global and regional ecosystem parameters of a comprehensive global three-dimensional ocean carbon cycle model and will be complementary to previous regional studies such as those by Losa et al. [2004], Hemmings et al. [2004], or Friedrichs [2002]. The first two papers indicate that ecosystem parameters in the North Atlantic region cannot be assumed invariant by using data assimilation experiments. For the Equatorial Pacific, Friedrichs [2002] explored how the assimilation of biological data into an ecosystem model can be used to distinguish between physical and ecological regime shifts and thus may identify shortcomings in the model formulation. Such findings have been confirmed by, for example, Garcia-Gorriz et al. [2003] who showed that the assimilation of Sea-viewing Wide Field-of-view Sensor (SeaWiFS) data of the Adriatic Sea into a NPZ/primitive equations model produces better fits to plankton bloom than to nonbloom conditions. Natvik and Evensen [2003] examined the sensitivity of the dynamical error of the

<sup>1</sup>Department of Atmospheric Oceanic and Space Sciences, University of Wisconsin-Madison, Madison, Wisconsin, USA.

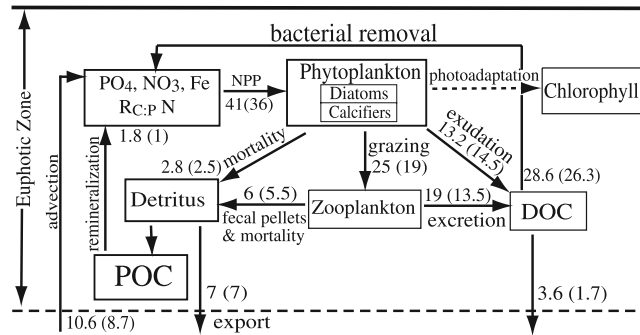


**Figure 1.** Schematic diagram of main processes simulated in the ecosystem model. Carbon fluxes between boxes are given in  $\text{Pg C yr}^{-1}$  (simulated value using optimized parameterization from regional assimilation experiment, RANC, RATC, and RASC, are given in parentheses, and values outside the parentheses represent values prior to the assimilation).

ecosystem model to the actual model state using the Ensemble Kalman Filter and SeaWiFS observations.

[4] In this study, an adjoint global three-dimensional carbon cycle model has been developed and applied to explore how globally uniform and regionally varying ecosystem parameters influence the optimization, and how assimilation of data from different seasons influence the solution. The response of the chlorophyll concentration and carbon fluxes with respect to selected ecosystem parameters will be quantitatively assessed as well. The objective of this study is to (1) test the applicability of the adjoint method in optimizing three-dimensional ecosystem parameters and reducing the model-data misfit, (2) analyze the performance of the optimization when SeaWiFS and WOA observation are assimilated, and to (3) discuss the uncertainties and limitation associated with the assimilation method adopted (e.g., in respect to the cost function formulation and multiple minima). In the following section, the ocean biogeochemical model used in this study is briefly described. Section 3 explains the satellite and in situ observations applied in the assimilation, followed by a description of the implementation of the inverse method in section 4. Results of the data assimilation experiments conducted in this study are presented in section 5. Section 6 provides an overall summary and discussion, and the paper concludes in section 7.

## 2. Model Description

[5] The ocean model used in this study is an ocean general circulation model coupled with a carbon cycle model. The model adopts the  $72 \times 72$  E grid [Arakawa and Lamb, 1977] (approximately  $3.5^\circ \times 3.5^\circ$  horizontal resolution), and contains 22 vertical layers with realistic bathymetry. The ocean general circulation model is the Hamburg Large-Scale Geostrophic (LSG) model [Maier-Reimer and Hasselmann, 1987; Maier-Reimer et al., 1993] and the carbon cycle model is the Hamburg Ocean Model of the Carbon Cycle (HAMOCC5.1) [Maier-Reimer, 1993; Six and Maier-Reimer, 1996; Aumont et al., 2003]. The LSG

model has been part of the Ocean-Carbon-Cycle Model Intercomparison Project (OCMIP) [Orr et al., 2001] and includes improved parameterizations of the mixed-layer and eddy-induced tracer transport [Gent et al., 1995; Visbeck et al., 1997] (see Mikolajewicz et al. [2006] for details). In a first order and with these revisions, the errors by shortcomings of the physical approximations are far lower than those of the biogeochemical formulations.

[6] A three-dimensional carbon cycle model (HAMOCC5.1) is coupled online to the LSG. The carbon cycle model includes 36 tracers and a nutrient, phytoplankton, zooplankton, and detritus NPZD-type ecosystem model (Figure 1). The initial condition of the HAMOCC5.1 model is based on a model used by Howard et al. [2006], which has been integrated for 10,000 years on an NEC supercomputer at the German Climate Modeling Center (DKRZ) in Hamburg. Detailed description of the HAMOCC5.1 used in this study is given by Howard et al. [2006] and in auxiliary Text S1<sup>1</sup>.

## 3. Observations

[7] Five-year seasonal climatology of SeaWiFS Level 3 chlorophyll data [Gregg and Casey, 2004], provided by NASA's Ocean Color Research Team (Goddard Earth Sciences Distributed Active Archive Center, <http://oceancolor.gsfc.nasa.gov>) are used for data assimilation in this study. To capture the seasonal pattern of the global ocean chlorophyll patterns, the weekly data from January 1998 through December 2003 are averaged for the four seasons, which are winter (January to March; JFM), spring (April to June; AMJ), summer (July to September; JAS), and fall (October to December; OND) and interpolated to the model grid (Figure 2). The coastal observations are excluded owing to the coarse resolution of the model and because of the different algorithms used by the satellite to measure open-ocean and coastal chlorophyll (case 1 and case 2 water) [Gordon and Morel, 1983]. We note that uncertainties of remote sensing chlorophyll data can be as high as  $\sim 30\%$  [McClain et al., 1998; O'Reilly et al., 2000; Gregg and Casey, 2004]. In addition to the remotely sensed chlorophyll data, we also use the seasonal in situ surface nitrate data provided by the WOA. The data is integrated between 0 and 50 meter depths to be assimilated into the model's topmost layer.

## 4. Inverse Method

### 4.1. Adjoint Method

[8] The adjoint model allows us to systematically estimate the sensitivity of the gradient of the cost function (i.e., calculates the model-data misfit) with respect to perturbation of the ecosystem parameter sets under the assumption that the model's functions are differentiable. Moreover, the adjoint model is very efficient (i.e., only a single forward and backward integration is needed) in finding the leading sensitivity of the model output with respect to multiple or large sets of parameters [Errico, 1997]. The adjoint model

<sup>1</sup>Auxiliary materials are available at <ftp://ftp.agu.org/apend/gb/2006GB002745>.

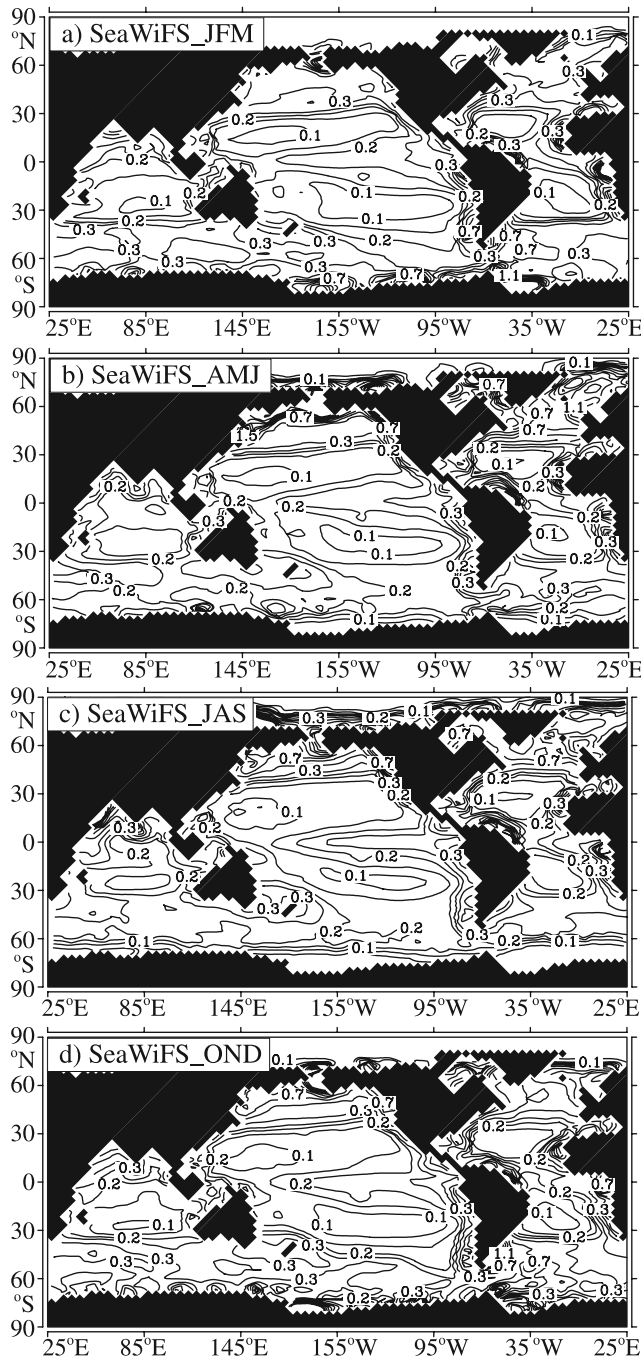


**Figure 2.** Averaged seasonal SeaWiFS chlorophyll data (in  $\text{mg Chl-a m}^{-3}$ ) for the months of (a) JFM, (b) AMJ, (c) JAS, and (d) OND. Isolines are at 0.05, 0.1, 0.15, 0.2, 0.25, 0.3, 0.5, 0.7, 0.9, 1.1, and 1.3.

can be developed with adjoint of the forward model code as shown, for example, by Talagrand [1991]. Here the adjoint codes have been generated by the TAMC (Tangent linear and Adjoint Model Compiler) [Giering and Kaminski, 1998] ([www.fastopt.com](http://www.fastopt.com)) and improved manually to be computationally efficient. The accuracy of the adjoint code has been tested using a finite difference (Taylor Series) approximation (see auxiliary Figure S7). A Quasi-Newton

descending algorithm M1QN3 by Gilbert and Lemaréchal [1989] is applied to minimize the cost function.

[9] The main idea behind the parameter optimization consists of four steps (Figure 3a). First, the forward model is integrated using a predefined set of control parameters. Secondly, the cost function computes the model-data difference. In the third step, the adjoint model determines the gradient of the cost function with respect to the control parameters. Finally, a descent algorithm is applied to the gradient of the cost function to compute a new set of control parameters that will return a reduced cost function. This routine is iterated until the cost function is sufficiently small or until the maximum number of iterations is reached. The result of the iterative process is an optimized set of control parameters with a minimized cost function. In practice, the shape of the cost function is very difficult to estimate, and owing to the nonlinearity of the model, it is very likely that multiple minima will exist [Schartau et al., 2001]. Conse-

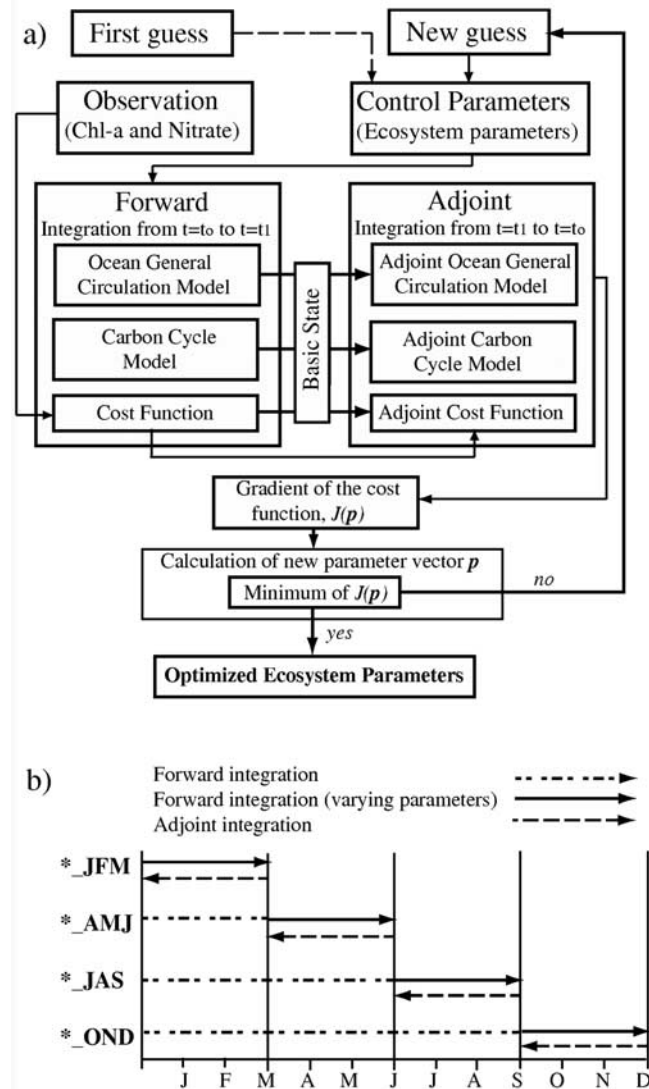


**Figure 3.** (a) Schematic flow diagram of the adjoint method parameter optimization and (b) schematic forward and backward integration for each season.

**Table 1.** Descriptions of the Selected Control Parameters Used in the Assimilation

$P_i$	Symbol	Description	Value	Units
P1	$lo$	POC remineralization rate	0.0033	$d^{-1}$
P2	$\gamma Z$	DOC excretion by ZOO	0.06	$d^{-1}$
P3	$dp$	PHY mortality rate	0.008	$d^{-1}$
P4	$\gamma P$	DOC excretion by PHY	0.06	$d^{-1}$
P5	$(1 - \varepsilon_{her})$	herbivore egestion as fecal pellets	(1 - 0.8)	-
P6	$go$	ZOO grazing rate	0.5	$d^{-1}$
P7	$zinges$	assimilation efficiency	0.5	-
P8	$dz$	ZOO mortality rate	0.008	$d^{-1}$
P9	$(1 - \varepsilon_{can})$	carnivore egestion as fecal pellets	(1 - 0.95)	-
P10	$do$	DOC maximum remineralization	0.005	$d^{-1}$

quently, it is important to note that not all of the minima reached in this study are the global minimum.

#### 4.2. Control Variables and Cost Function

[10] The control vector  $\tilde{\mathbf{p}}$  consists of the ten ecosystem control variables  $P_i$  (Table 1), which are selected on the basis of previous sensitivity tests (see auxiliary Figure S1). Since values of these control variables  $P_i$  range over several orders of magnitude, their values are scaled to  $P_i' = [P_i \text{ (new guess)}] / [P_i \text{ (first guess)}]$  [e.g., Giering, 1989; Friedrichs, 2001] to avoid precision problems with the data assimilative model. The scaled control variables  $P_i'$  of the control vector  $\tilde{\mathbf{p}}'$  are therefore all nondimensional with equal orders of magnitude. In general, the cost function measures the quadratic misfit between simulated surface chlorophyll,  $m_{i,j}(\tilde{\mathbf{p}}')$ , and the observations,  $x_{i,j}$ :

$$J(\tilde{\mathbf{p}}') = \frac{\sum_{i,j} W_{i,j} [x_{i,j} - m_{i,j}(\tilde{\mathbf{p}}')]^2}{\sigma_{i,j}^2}. \quad (1)$$

The subscripts  $i$  and  $j$  represent the grid location in the x and y directions. Here  $\sigma$  represents the scale factor and the weight term of each grid point,  $W_{i,j}$ , is calculated on the basis of the volume ( $V_{i,j}$ ) of each model grid cell,

$$W_{i,j} = \frac{V_{i,j}}{\sum_{i,j} V_{i,j}}, \quad (2)$$

where the equatorial (polar) regions have the largest (smallest) weight for the cost function. This is because equatorial model grids represent a larger surface area than the higher-latitude model grids. We note that the cost function only calculates the tracer misfit in the surface (i.e., top layer in the model).

[11] One of the many uncertainties associated with the adjoint method is the formulation of the cost function (i.e., the selection of the scale factor  $\sigma$  and weight term in the cost function may significantly alter the final solution). Various choices of  $\sigma$  have been used in the past, but there was no specific study investigating the implication of the different value chosen for  $\sigma$  [Evans, 2003; Oeschlies, 2006]. In order to choose the most efficient cost function, a set of a priori identical twin experiments (see section 5.1 for identical twin experiment description) has been conducted to analyze the role of scale factor and weight term in the cost function. Three different values of  $\sigma_{i,j}$  are tested using similar minimization

technique. The scale factor in the first experiment is set to be a uniform constant of averaged model chlorophyll variance

$$\sigma_{i,j} = 0.2 \text{ mg Chl} - a \text{ m}^{-3}. \quad (3)$$

In the second experiment,  $\sigma_{i,j}$  is set to be spatial variance as a function of observation

$$\sigma_{i,j} = 0.3 * x_{i,j}. \quad (4)$$

In the third experiment, the scale factor is set to be spatial model variance at every grid point

$$\sigma_{i,j} = \text{var}(x_{i,j}). \quad (5)$$

All of the assimilations are conducted with the same initial condition and the identical twin experiments are run for the JFM months. Finally, a universal cost function (will be referred to assess function) is used at the end to measure the performance of all assimilation. The assess function is defined as

$$A(\tilde{\mathbf{p}}') = \frac{\sum_{i,j} [x_{i,j} - m_{i,j}(\tilde{\mathbf{p}}')]^2}{(0.3 * x_{i,j})^2}. \quad (6)$$

The assess function is formulated on the basis of 30% observation error limit associated with SeaWiFS chlorophyll. To analyze the role of the weight term, three additional, similar experiments are conducted in which the weight term in the cost function are set to one.

[12] Table 2 describes and summarizes the results of the six experiments together with the a priori and a posteriori value for both the cost and assess functions. The role of the weight term is obvious. When the weight term is neglected, the high-latitude regions do slightly better than if the weight term is included. The opposite is true for the tropical regions (see auxiliary Figure S2). The best reduction in the assess function is returned by experiment EXP\_COSTA, where the scale factor is set to be constant and the weight term is included. The lowest performance returned by experiment EXP\_COSTC, where spatial model variance is used. Furthermore, more control parameters are recovered when a constant scale factor is adopted (see auxiliary Table S1). These experiments show that for the given model and assimilation method, an inclusion of regional weight term and a constant value for the scale factor in the cost function

**Table 2.** Comparison of A Priori and A Posteriori Values for Both Cost and Assess Functions Based on Different Scale Factor and Weight Term in the Adopted Cost Function

Exp	$\sigma_{I_i}$	$J_O$	$J_T$	$(J_T/J_O)$	$A_O$	$A_T$	$(A_T/A_O)$
Exp_CostA	0.2	1.550e - 1	1.453e - 2	0.0938	1.034e + 4	1.974e + 3	0.1909
Exp_CostB	$0.3 * x_{i,j}$	2.554e + 0	6.027e - 1	0.2360	1.034e + 4	2.345e + 3	0.2268
Exp_CostC	$\text{var}(x_{i,j})$	2.567e + 5	7.778e + 4	0.3030	1.034e + 4	5.956e + 3	0.5760
Exp_CostA_NW	0.2	7.354e + 2	6.494e + 1	0.0883	1.034e + 4	2.096e + 3	0.2027
Exp_CostB_NW	$0.3 * x_{i,j}$	1.034e + 4	2.550e + 3	0.2467	1.034e + 4	2.550e + 3	0.2466
Exp_CostC_NW	$\text{var}(x_{i,j})$	1.562e + 9	2.732e + 8	0.1748	1.034e + 4	5.085e + 3	0.4918

is more likely to return the maximum reduction in the cost function.

## 5. Experiment Design and Results

[13] Five classes of data assimilation experiments have been carried out with the LSG-HAMOCC5.1 model to improve the seasonal chlorophyll forecast (see Table 3). Each class of experiments consists of four experiments

(12 experiments for regional assimilation, see section 5.4), one for each season. For each of those experiments, the corresponding seasonal (JFM, AMJ, JAS, and OND) climatological data are assimilated into the model. All experiments have been initialized with the same initial condition (December climatology) and control variables have only been altered for the season in which data has been assimilated into the model. For example, for the OND assimilation, the control parameters use fixed reference values for

**Table 3.** Experiment Description, Setups, and Cost Function Reduction for Each Experiment<sup>a</sup>

Experiments	Data	Optimized Parameters		Cost Function Reduction
		Months	Regions	
REF	-	-	-	-
ITE_JFM	Synthetic Chl-a (noise)	JFM	global	92%
ITE_AMJ	Synthetic Chl-a (noise)	AMJ	global	66%
ITE_JAS	Synthetic Chl-a (noise)	JAS	global	36%
ITE_OND	Synthetic Chl-a (noise)	OND	global	63%
ITEN_JFM	Synthetic Chl-a (no noise)	JFM	global	94%
ITEN_AMJ	Synthetic Chl-a (no noise)	AMJ	global	95%
ITEN_JAS	Synthetic Chl-a (no noise)	JAS	global	82%
ITEN_OND	Synthetic Chl-a (no noise)	OND	global	97%
GAC_JFM	SeaWiFS Chl-a	JFM	global	1%
GAC_AMJ	SeaWiFS Chl-a	AMJ	global	12%
GAC_JAS	SeaWiFS Chl-a	JAS	global	16%
GAC_OND	SeaWiFS Chl-a	OND	global	18%
GACN_JFM	SeaWiFS Chl-a and NO <sub>3</sub>	JFM	global	9%
GACN_AMJ	SeaWiFS Chl-a and NO <sub>3</sub>	AMJ	global	12%
GACN_JAS	SeaWiFS Chl-a and NO <sub>3</sub>	JAS	global	17%
GACN_OND	SeaWiFS Chl-a and NO <sub>3</sub>	OND	global	17%
RANC_JFM	SeaWiFS Chl-a	JFM	north	17%
RANC_AMJ	SeaWiFS Chl-a	AMJ	north	20%
RANC_JAS	SeaWiFS Chl-a	JAS	north	54%
RANC_OND	SeaWiFS Chl-a	OND	north	43%
RATC_JFM	SeaWiFS Chl-a	JFM	tropic	3%
RATC_AMJ	SeaWiFS Chl-a	AMJ	tropic	1%
RATC_JAS	SeaWiFS Chl-a	JAS	tropic	12%
RATC_OND	SeaWiFS Chl-a	OND	tropic	8%
RASC_JFM	SeaWiFS Chl-a	JFM	south	9%
RASC_AMJ	SeaWiFS Chl-a	AMJ	south	28%
RASC_JAS	SeaWiFS Chl-a	JAS	south	3%
RASC_OND	SeaWiFS Chl-a	OND	south	38%
RANCG_JFM	SeaWiFS Chl-a	JFM	north	17%
RANCG_AMJ	SeaWiFS Chl-a	AMJ	north	20%
RANCG_JAS	SeaWiFS Chl-a	JAS	north	14%
RANCG_OND	SeaWiFS Chl-a	OND	north	1%
RATCG_JFM	SeaWiFS Chl-a	JFM	tropic	7%
RATCG_AMJ	SeaWiFS Chl-a	AMJ	tropic	1%
RATCG_JAS	SeaWiFS Chl-a	JAS	tropic	22%
RATCG_OND	SeaWiFS Chl-a	OND	tropic	8%
RASCG_JFM	SeaWiFS Chl-a	JFM	south	8%
RASCG_AMJ	SeaWiFS Chl-a	AMJ	south	29%
RASCG_JAS	SeaWiFS Chl-a	JAS	south	18%
RASCG_OND	SeaWiFS Chl-a	OND	south	44%

<sup>a</sup>The northern, tropical, and southern regions are defined as 90°N–22°N, 22°N–22°S, and 22°S–90°S, respectively.

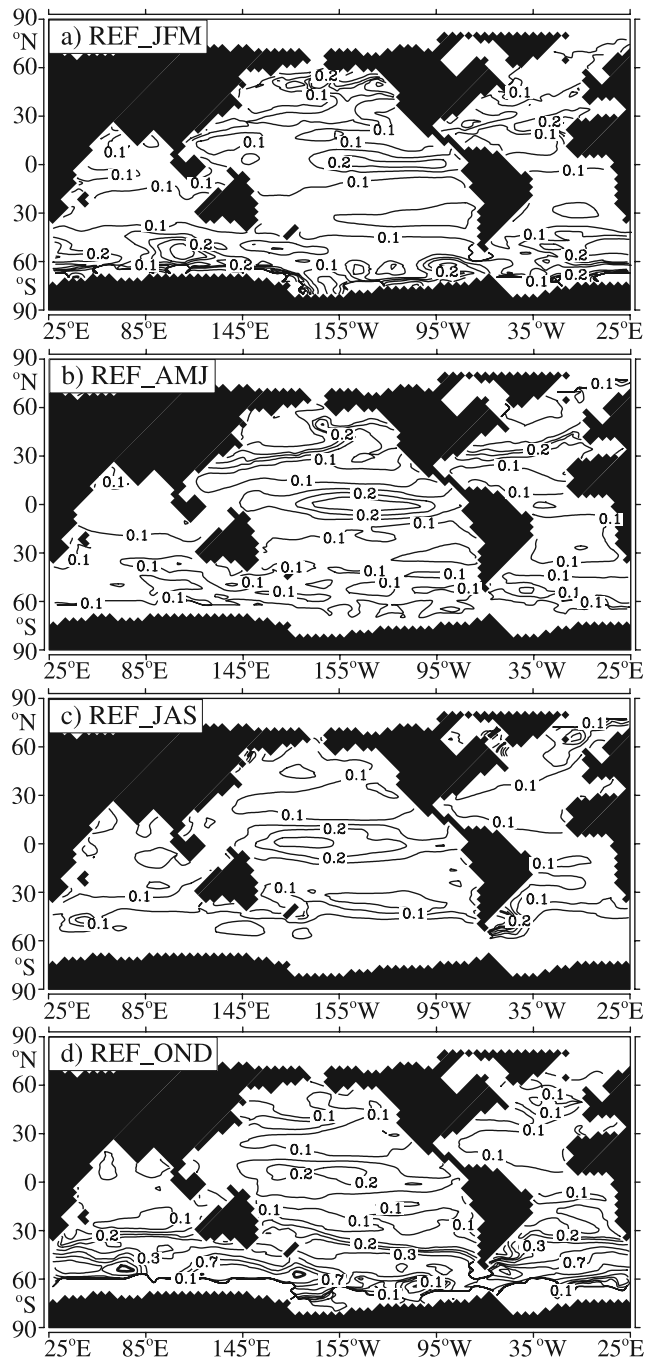


**Figure 4.** Model simulated “first guess” (reference run) seasonal surface chlorophyll concentration (in  $\text{mg Chl-a m}^{-3}$ ) for the months of (a) JFM, (b) AMJ, (c) JAS, and (d) OND. Isolines are at 0.05, 0.1, 0.15, 0.2, 0.25, 0.3, 0.5, 0.7, 0.9, 1.1, and 1.3.

January to September and are only varied (optimized) for the fall season (OND) (see Figure 3b). The seasonal chlorophyll concentration produced by the model using the first guess parameter (reference) vector  $\tilde{p}$  is shown in Figure 4.

[14] The first class of experiments is aimed at estimating the sensitivity of the simulated chlorophyll concentration to changes in ecosystem parameters by conducting identical

twin experiments (ITE). In the second class of experiments (GAC), SeaWiFS seasonal climatological chlorophyll data are assimilated into the adjoint model to optimize the parameter vector  $\tilde{p}$  for the global ocean. In the third class of experiments (GACN), nitrate data from the WOA is included as an additional constraint in the assimilation. In the fourth class of experiments (RAC), the global ocean is divided into three regions: northern ( $90^{\circ}\text{N}-22^{\circ}\text{N}$ ), tropical ( $22^{\circ}\text{N}-22^{\circ}\text{S}$ ), and southern ( $22^{\circ}\text{S}-90^{\circ}\text{S}$ ) regions. This class of experiments is divided into three subclasses of experiments, a subclass for each region (i.e., there are 12 separate assimilations for RAC). For each region and season, SeaWiFS chlorophyll data is assimilated into the three-dimensional model in order to analyze the sensitivity of simulated chlorophyll in different regions and seasons. The performance of each experiment is summarized in Table 3. To investigate the sensitivity of the phytoplankton growth parameters, a fifth class of experiment is added, which is similar to the fourth class experiment, but include a variation of the temperature-dependent phytoplankton growth parameters.

### 5.1. Class of Identical Twin Experiments (ITE)

[15] The ITE is applied to test the robustness of the adjoint method [Friedrichs, 2001]. In the ITE, a model reference run (REF) has been carried out for each season using a reference parameter set. The outputs of the simulated chlorophyll concentration from these simulations have been perturbed by Gaussian noise to generate the synthetic data, which are used for data assimilation. The Gaussian noise has been generated for each location by a Gaussian random function multiplied by 30% of the local simulated chlorophyll concentration. The magnitude of the Gaussian noise is comparable to the uncertainty of the SeaWiFS data (section 3). As an initial condition for the data assimilation, the parameters  $P_i$  in  $\tilde{p}$  have been perturbed by a factor of 0.9 of their initial value without noise. Thus a good recovery of the parameter after assimilation of the synthetic data would yield the parameter’s value similar to the reference run (which are the unperturbed parameters).

[16] Experiments with noise (i.e., ITE\_JFM, ITE\_AMJ, ITE\_JAS, and ITE\_OND) demonstrated that the model simulated chlorophyll concentration is significantly sensitive with respect to five (P2, P4, P5, P6, and P7) of the ten parameters. Some of these parameters were able to recover close to their initial values. The cost function was significantly reduced, for example by 92% in the JFM experiment. To analyze the spatial distribution of model-data misfit, we introduce relative cost function term

$$j_{ij} = \sqrt{\frac{[x_{ij} - m_{ij}(\tilde{p})]^2}{[0.3 \cdot x_{ij}]^2}} \quad (7)$$

The relative cost function gives the model-data chlorophyll misfit at each grid point and divides it by 30% of the data value, which is the approximation accuracy of the SeaWiFS observation. The a priori and a posteriori relative cost function plot for the ITE\_JFM experiments are shown in Figure 5, which shows significant global reduction in

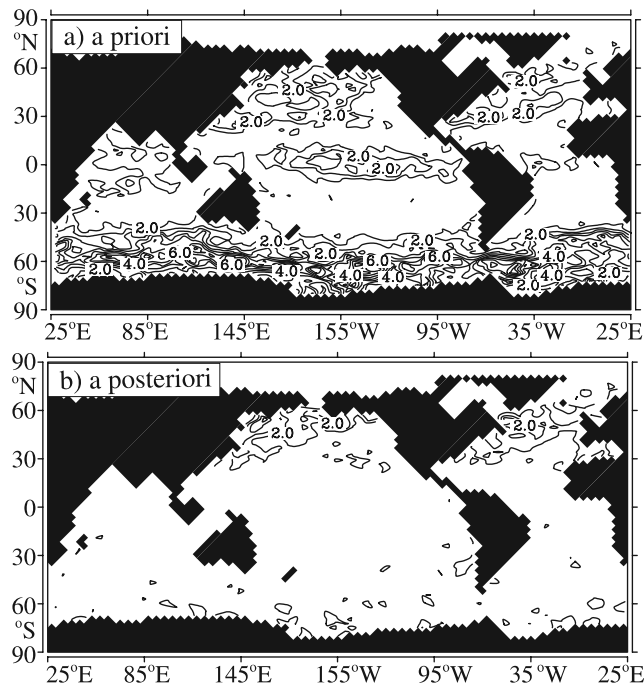


**Figure 5.** (a) A priori and (b) a posteriori relative cost function plot of the ITE\_JFM identical twin experiment with noise added to the artificial data. Isolines are at 1, 2, 3, 4, 5, 6, and 7.

relative cost function, thus the performance of the identical twin experiments demonstrates that the applicability of the adjoint method is sufficient as a means to reduce model-data misfit.

[17] To test whether the noise is the reason for the non-recovered optima parameters, we conducted an additional ITE experiment set where no noise is added (ITEN\_JFM, ITEN\_AMJ, ITEN\_JAS, and ITEN\_OND). The ITE experiments without noise yield better reduction in the cost function over all seasons (see Table 3 and Figure 6) than experiments with noise. Despite the significant reduction in model-data misfit, some parameters remain unable to recover their initial value (see auxiliary Table S1), which is likely related to the nonlinearity of the problem and thus resulted in multiple minima in the cost function. The condition number of the Hessian matrix (as approximated by the M1QN3), which is the ratio of the smallest to the largest eigenvalues of a symmetric positive Hessian matrix, is close to unity (1.0269). This indicates that the cost function is steep-shaped and the minimizations converge quickly [Thacker, 1989], on average about 5 iterations for all ITE experiments. We note that the estimate of the Hessian matrix of M1QN3 has substantial uncertainties related to the approximation in a nonlinear system.

## 5.2. Class of Global Assimilation of SeaWiFS Chlorophyll Experiment (GAC)

[18] In this class of experiments, climatological SeaWiFS chlorophyll observations are assimilated into the LSG-HAMOCC5.1 for each season. The ecosystem parameters are optimized for a set of globally uniform values. Optimal

model solutions resulting from the experiment GAC showed very small reductions in the cost function: 1%, 12%, 16%, and 18% for JFM, AMJ, JAS, and OND months, respectively. Most of this reduction occurred in the high latitudes, which is related to the large a priori model-data bias in high latitudes [Tjiputra, 2004]. The optimal solution indicates a seasonal variability of the chlorophyll concentration, which is high in the Southern Ocean during OND, and in the North Pacific and North Atlantic during JAS. A higher concentration of chlorophyll is produced in the northern Atlantic and Pacific for AMJ and JAS in the optimized model runs. Small improvement occurred in the Southern Ocean. The model-data bias in the Equatorial Indian and Atlantic were reduced, but significant differences remain in the Equatorial Pacific region.

[19] In the JFM months' assimilation, significant model-data bias remained, with a nearly identical a priori and a posteriori model-data misfit. The condition number of the Hessian matrix for the GAC\_JFM assimilation of 2.25367 is larger than that of the ITE experiment, implying a flatter cost function and slower convergence of the cost function (after 25 iterations). This low reduction in the cost function may be related to the differences between the model and data of nitrate concentrations in the high-latitude regions. For example, the model underestimates the nitrate concentrations in the Southern Ocean during the JFM season. In the OND assimilation, the a priori model-data discrepancies are mostly concentrated in the high latitudes and the assimilation reduced this misfit especially in the Southern Ocean significantly. However, at the same time, it increased the misfit at tropical and northern high latitudes (see

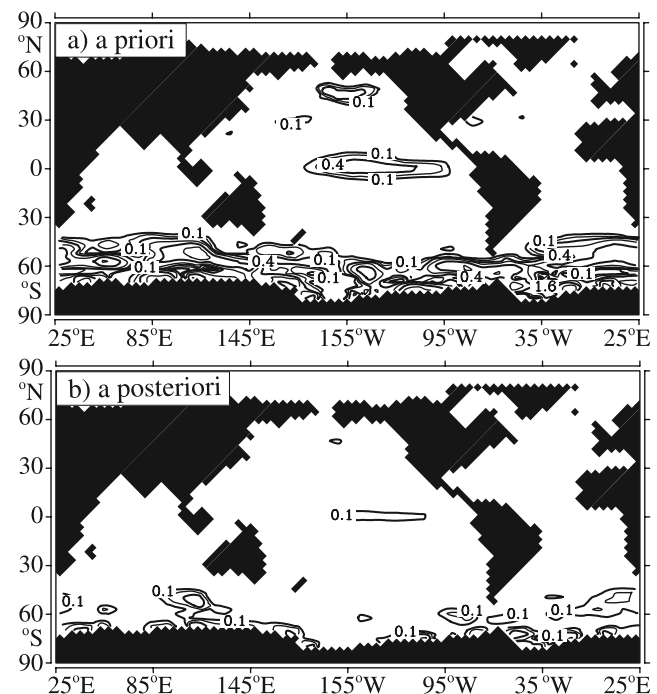


**Figure 6.** (a) A priori and (b) a posteriori relative cost function of the ITEN\_JFM experiment where no noise was added. Isolines are at 0.1, 0.2, 0.4, 0.8, 1.6, and 3.2.

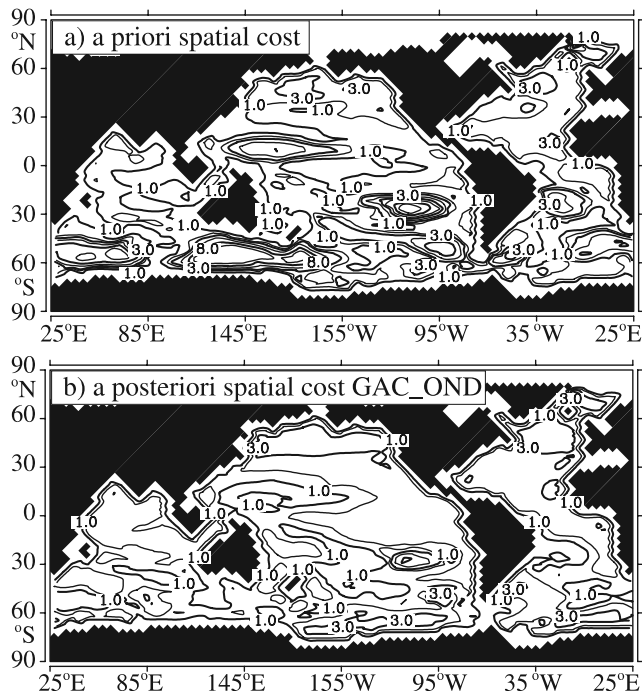


**Figure 7.** (a) A priori and (b) a posteriori cost function plots of the GAC\_OND assimilation divided by 30% of the observational value. Isolines are at 1, 2, 3, 5, 8, 11, and 15.

Figure 7). This occurred mainly because of the model a priori overestimates of the chlorophyll concentration in the Southern Ocean. The optimized parameter sets reduced the overall phytoplankton mass by increasing the phytoplankton exudation rate from 0.06 to 0.08 and grazing rate from 0.5 to 0.6 per day. These outcomes suggest that different parameterizations may be needed for different regions (latitudes). All of the seasonal SeaWiFS assimilations, excluding the OND, proposed having a lower herbivore egestion rate (P5), zooplankton grazing rate (P6), and assimilation efficiency (P7).

### 5.3. Class of Global Assimilation of SeaWiFS Chlorophyll and WOA Nitrate Experiment (GACN)

[20] In this experiment, the seasonal nitrate data from the World Ocean Atlas were included in the assimilation as an additional constraint on the cost function. Hence the updated cost function becomes

$$J(\tilde{\mathbf{p}}) = J_{CHL} + J_N = \frac{\sum_{i,j} W_{i,j} [x_{i,j} - m_{i,j}(\tilde{\mathbf{p}})]^2}{\sigma_{chl}^2} + \frac{\sum_{i,j} W_{i,j} [y_{i,j} - n_{i,j}(\tilde{\mathbf{p}})]^2}{\sigma_{NO_3}^2}, \quad (8)$$

where  $y_{i,j}$  and  $n_{i,j}(\tilde{\mathbf{p}})$  represent observation and model-generated nitrate concentrations, respectively, and  $\sigma_{NO_3}$  represents the uniform standard deviation of nitrate ( $4.0 \mu\text{mol N L}^{-1}$ ). In this experiment, the global observations of nitrate and chlorophyll are assimilated together to reduce the model-data bias of both nitrate and chlorophyll concentrations.

[21] Overall, the assimilation performance of GACN is slightly better than GAC (see Table 3). The total cost function value ( $J_{TOT} = J_{CHL} + J_N$ ) for the GACN\_JFM assimilation is reduced by 9% after only six iterations. Both  $J_{CHL}$  and  $J_N$  are also reduced by 9%. Experiment

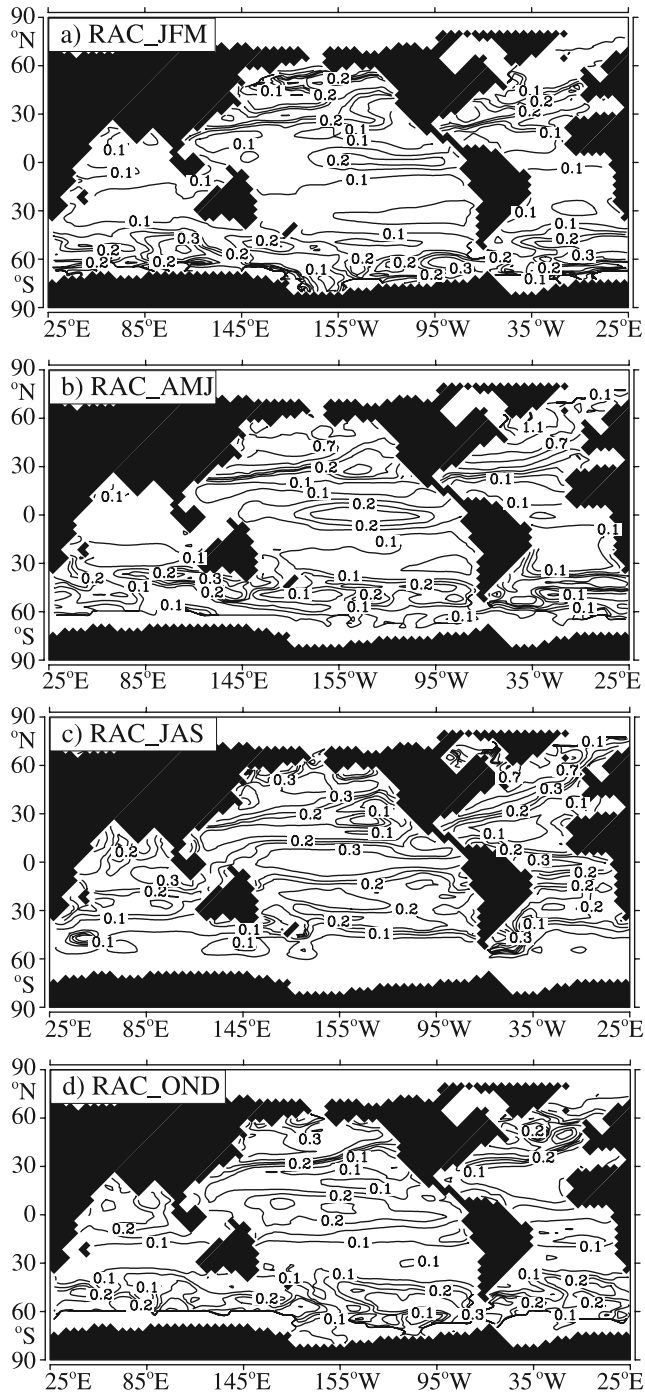


**Figure 8.** Model simulation of chlorophyll (in  $\text{mg Chl-a m}^{-3}$ ) using optimized parameters from regional assimilations of (a) RAC\_JFM, (b) RAC\_AMJ, (c) RAC\_JAS, and (d) RAC\_OND. Isolines are at 0.05, 0.1, 0.15, 0.2, 0.25, 0.3, 0.5, 0.7, 0.9, 1.1, and 1.3.



**Table 4.** A Posteriori Ecosystem Parameters<sup>a</sup>

Experiments	P1'	P2'	P3'	P4'	P5'	P6'	P7'	P8'	P9'	P10'
(A priori)	1.000	1.000	1.000	1.000	1.000	1.000	1.000	1.000	1.000	1.000
RANC_JFM	1.000	1.065	0.981	0.787	0.910	0.888	0.924	1.012	1.000	1.028
RATC_JFM	1.007	1.064	0.997	0.936	0.954	0.928	0.904	1.015	1.005	1.062
RASC_JFM	1.000	1.027	1.000	0.988	0.970	0.975	0.976	1.005	1.000	1.003
RANC_AMJ	1.000	1.079	0.972	0.479	0.774	0.840	0.840	1.016	1.000	1.065
RATC_AMJ	1.000	1.001	1.000	0.999	0.999	0.999	0.998	1.000	1.000	1.000
RASC_AMJ	1.002	1.114	0.991	0.845	0.888	0.845	0.910	1.022	1.002	1.028
RANC_JAS	1.002	1.781	0.958	0.298	0.100	0.198	0.100	1.148	1.020	1.247
RATC_JAS	1.003	1.216	0.997	0.914	0.798	0.810	0.746	1.041	1.014	1.035
RASC_JAS	0.998	1.100	0.995	0.862	0.929	0.879	0.960	1.019	0.994	0.978
RANC_OND	1.000	1.304	0.968	0.847	0.918	0.774	0.772	1.053	1.030	1.022
RATC_OND	1.000	1.090	1.000	0.980	0.960	0.930	0.920	1.020	1.010	1.010
RASC_OND	0.999	0.821	1.102	0.942	1.110	1.526	1.538	0.964	0.996	0.792
Mean	1.001	1.139	0.997	0.823	0.859	0.883	0.883	1.026	1.006	1.022
Variance	0.000	0.054	0.001	0.047	0.065	0.085	0.101	0.002	0.000	0.010

<sup>a</sup>See Table 1 for parameter descriptions. Values with mean and variance resulted from every regional assimilation experiments (RAC).

GAC\_JFM did not reach the minimum in the cost function, and the additional nitrate data improved the data assimilation performance. Similarly, there were improvements from experiment GAC for the GACN\_AMJ and GACN\_JAS assimilations. The additional constraint of nitrate did not improve the model-data bias in the Southern Ocean, which could be related to the low chlorophyll concentration in the model, especially during JAS. For the GACN\_OND assimilation, the additional nitrate data were able to reduce the model-data bias of chlorophyll concentration in the Southern Ocean, and the cost function did not increase in the tropics and northern regions, unlike in GAC\_OND.

#### 5.4. Class of Regional Assimilation of SeaWiFS Chlorophyll Experiment (RAC)

[22] There is evidence of biogeographical provinces [Longhurst, 1998] and previous modeling studies [Losa *et al.*, 2004; Sarmiento *et al.*, 2004; Dunne *et al.*, 2005; Hood *et al.*, 2006] have pointed out that different ocean regions have different biogeochemical characteristics and thus different sets of parameters. In a first approach, we examined the sensitivity of the simulated chlorophyll concentration to spatial varying parameters by dividing the ocean into low- and high-latitude regions: southern ( $>22^{\circ}\text{S}$ ), tropical ( $22^{\circ}\text{N}-22^{\circ}\text{S}$ ), and northern ( $>22^{\circ}\text{N}$ ) region. A total of twelve experiments were performed (see Table 3), one for each region and season. SeaWiFS data have been assimilated only in these specific regions, but the ecosystem parameters have been varied globally. The primary motivation of these experiments is to investigate the sensitivity of the regional chlorophyll concentration to the ecosystem parameters.

[23] The regional assimilations have an improved performance in comparison to the previous experiments, yielding overall reductions of the model-data misfit to 9%, 16%, 29%, and 35% for JFM, AMJ, JAS, and OND, respectively. The a posteriori seasonal chlorophyll model simulation using regionally and seasonally varying ecosystem parameters are shown in Figure 8. The a posteriori regional ecosystem parameter values are shown in Table 4. The most significant improvement took place in the summer northern region in the RANC\_JAS assimilation, where the

cost function was reduced by more than half (54%). This, however, required a large reduction of the zooplankton grazing rate ( $\sim 0.1 \text{ d}^{-1}$ ) and the assimilation efficiency (0.05) parameter. It is possible that the relatively low grazing rate produced in the RANC\_JAS experiment is due to the very high chlorophyll concentration observed by SeaWiFS in the North Atlantic regions. Chester [2000] claimed that these large phytoplankton blooms in the North Atlantic region during the spring and early summer are associated with the excess of production by phytoplankton over the low consumption (zooplankton grazing) following the development of a thermocline and increasingly favorable light conditions. Another significant cost function reduction in the northern region occurred in the RANC\_OND assimilation (43%), where the optimized parameter values were able to replicate the high chlorophyll concentration observed in the North Atlantic and North Pacific. In the tropical regions, the cost function is reduced by an average of only  $\sim 6\%$ . The only notable model improvement is shown in the RATC\_JAS simulation, with a 12% cost function reduction, where the optimized parameter values increase the chlorophyll concentration in the Equatorial Indian and Equatorial Atlantic. This relatively low reduction in the cost function may be due to the more linear physical processes in the tropics (e.g., low seasonal variability in temperature and light, and no sea ice formation) than in the higher-latitude regions. In the southern region, the assimilation of the SeaWiFS observations into the model for RASC\_OND improved the predictions substantially (38% cost function reduction), but the model-data bias of chlorophyll concentration for RASC\_JAS remains high (only 8% cost function reduction), which is due the very low initial chlorophyll concentration.

[24] Table 4 lists the variances of each of the control variables with the highest variances for P2, P4, P5, P6, and P7, which is consistent with the ITE simulations in section 5.1. Optimal parameters in the tropical regions have lower variances than parameters in the high-latitude regions, implying that some parameters may be reformulated as a function of light, temperature, or mixed-layer depth. Overall, the data assimilation significantly improved the chlorophyll predictions for the high latitudes. The only noticeable

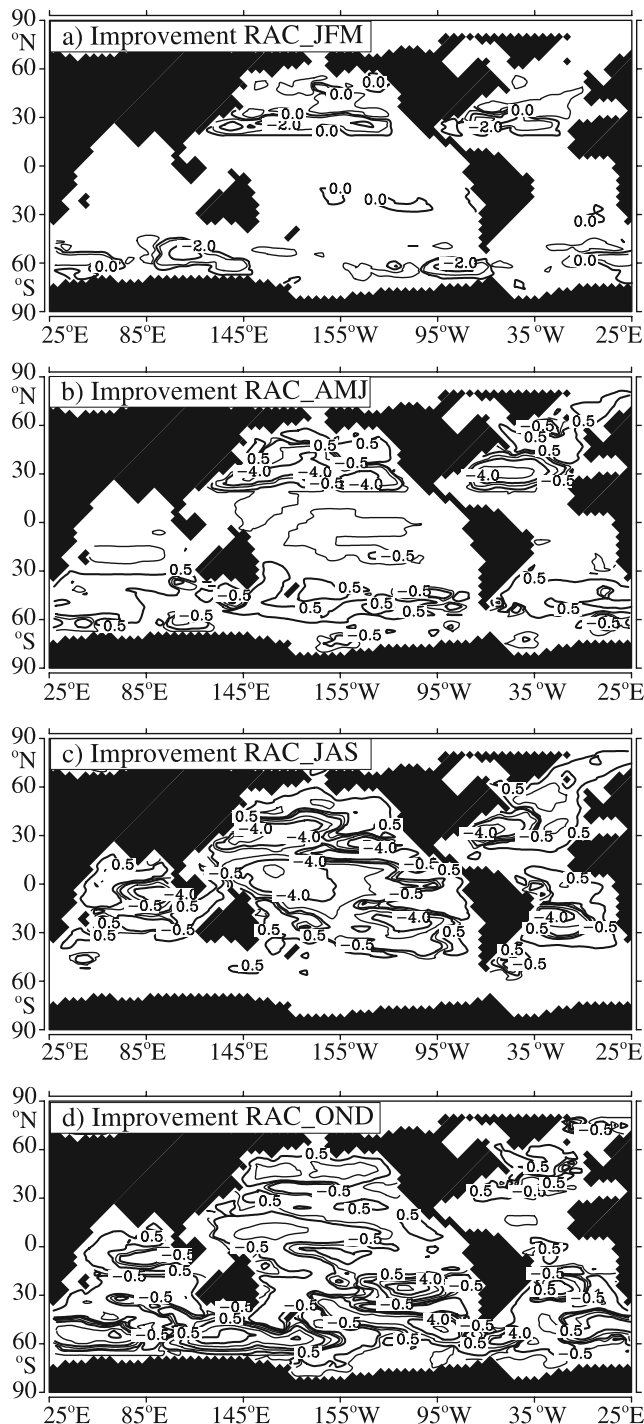


**Figure 9.** Difference plots between a priori and a posteriori cost function ( $j_{a\text{ priori}} - j_{a\text{ posteriori}}$ ) of regional assimilation experiments for the months of (a) JFM, (b) AMJ, (c) JAS, and (d) OND (positive values represent improvement of the model projection or reduction in model-data difference, while zero or negative values represent no improvement). Isolines are at  $-8$ ,  $-4$ ,  $-2$ ,  $-0.5$ ,  $0$ ,  $0.5$ ,  $2$ ,  $4$ ,  $8$ , and  $12$ .

improvements in the equatorial region occur in the RAC\_JAS assimilation (i.e., equatorial Indian, Atlantic, and eastern Pacific Ocean). The largest improvements occur in the Arctic and North Atlantic Ocean in the RANC\_JAS assimilation. The Southern Ocean was improved significantly in the RASC\_OND assimilation (see Figure 9).

[25] The annual carbon fluxes between main components yielded by the marine ecosystem model are shown in Figure 1. The a priori annual global net primary production is  $41 \text{ Pg C yr}^{-1}$ , which comprised of  $10.6 \text{ Pg C yr}^{-1}$  new and  $30.4 \text{ Pg C yr}^{-1}$  regenerated production. The a posteriori model run using the optimized ecosystem parameter set from RAC experiments reduced the new and regenerated production to  $8.7 \text{ Pg C yr}^{-1}$  and  $27.3 \text{ Pg C yr}^{-1}$ , respectively. The net primary production remains in the lower limit of annual NPP value suggested by *Antoine et al.* [1996] of  $36 \text{ Pg C yr}^{-1}$  (Figure 1), higher than *Berger's* [1989] value of  $27.6 \text{ Pg C yr}^{-1}$ , but relatively lower than that estimated by *Falkowski et al.* [1998] and *Behrenfeld et al.* [2005] of  $\sim 45\text{--}50$  and  $60 \text{ Pg C yr}^{-1}$ , respectively. The assimilation increases the chlorophyll concentration in most of the global regions, except for the Southern Ocean in the OND months. Accordingly, the net primary production for the JFM, AMJ, and JAS were increased by  $1.7$ ,  $0.6$ , and  $0.6 \text{ Pg C yr}^{-1}$ , respectively, but is reduced significantly by  $8 \text{ Pg C yr}^{-1}$  in the OND months. The a posteriori phytoplankton stock is relatively high because of the lower grazing rate (by zooplankton) parameter, thus the annual flux of carbon from phytoplankton to zooplankton compartment in the model were reduced by approximately  $6 \text{ Pg C yr}^{-1}$ . In a steady state, the new primary production is equal to the total export of organic material out of the euphotic zone. The new set of ecosystem parameters reduces the export of DOC out of the euphotic layer by nearly  $2 \text{ Pg C yr}^{-1}$ , while the export production of POC into the deep ocean is maintained at  $\sim 7 \text{ Pg C yr}^{-1}$ .

### 5.5. Class of Regional Assimilation of SeaWiFS Chlorophyll Experiment With Added Growth Parameters (RACG)

[26] To investigate the sensitivity of the simulated chlorophyll concentration to changes in the phytoplankton growth formulation, we varied parameters of the *Eppley* [1972] formula (detail growth formulation is given in auxiliary Text S1),

$$f(T) = a \cdot b^{cT} \quad (9)$$

This formulation seems to be a logical starting point for modeling phytoplankton growth since the maximum expected growth rate varies with temperature, but different taxonomic groups have different growth characteristics. Therefore, if dominant groups change over time, the parameters in (9) may be varied over space and time. Three growth-associated parameters (maximum growth parameter  $a$ , growth rate at  $0^\circ\text{C}$   $b$ , and temperature dependence of growth  $c$ ) are varied regionally and seasonally and these experiments are denoted RACG.

[27] The results of the assimilations (auxiliary Table S3) indicate that most of the experiments confirm the parameter

selection of *Eppley* [1972]. Five of the twelve experiments yield an decrease of the a posteriori model-data bias, but three of them yield an increase of the a posteriori model-data bias compare to the RAC experiments (see auxiliary Table S3 for list of optimized parameter values). Most of the optimized parameters, which deviate noticeable from the previous assimilation, are most likely because the minimization move toward different direction in the cost function. For example, eight parameters of RANC\_OND, which produced a 43% reduction in the cost function, deviate significantly from experiment RANCG\_OND, which only yielded a 7% reduction in the cost function. Table 3 summarizes the performance of all assimilation experiments. This class of experiment shows that it is not obvious whether adding more control parameters in the assimilation would further reduce the cost function.

[28] To test the sensitivity model long-term integration toward the control parameters, we run two 10-year forward model integrations, one using the a priori, and one using the optima control parameters. The chlorophyll concentrations from the 10-year runs are seasonally averaged, and the spatial model-data misfit for the JFM and JAS months are plotted in supplemental Figure 4. The model-data misfit is calculated using the relative cost function (equation (7)). Essentially, the new parameters effectively eliminate most of the model-data discrepancies in the northern and southern regions. However, in the tropical regions, the a posteriori model simulations perform poorly. We suspect this is due to the sluggish western boundary formulation in our model. This result further stresses the prospect of using regional parameter optimization following biogeographical provinces suggested by *Longhurst* [1998].

## 6. Summary and Discussions

[29] In this study, an adjoint three-dimensional marine biogeochemical model was developed and tested using identical twin experiments and by assimilating SeaWiFS chlorophyll and WOA nitrate observations. The next two subsections will discuss and evaluate the inverse method as well as the physical/biogeochemical aspect of this study.

### 6.1. Evaluation of Inverse Method

[30] Several factors influence the performance of the optimization, such as the selection of the scale factor,  $\sigma$ , in the cost function (see equation (1)). A selection of a spatially varying scale factor did not significantly improve the forecast as shown in Table 2. Also, changes in the formulation of the weighting term in the cost function may alter the results of the assimilation [*Losa et al.*, 2004], but this sensitivity is not confirmed by this study (see auxiliary Figure S2).

[31] In the identical twin experiments, the sensitivities of model output toward ecosystem parameters were investigated. The adjoint model was able to identify five of the selected ten parameters that are significantly more sensitive than the others: phytoplankton and zooplankton DOC exudation, herbivore egestion rate as fecal pellets, zooplankton grazing, and assimilation efficiency. In general, the identical twin experiments were able to recover, with a substantially reduced cost function by up to 92%, the

sensitive perturbed parameters, but did not do as well with the less sensitive ones. Assimilation of SeaWiFS chlorophyll data into the carbon cycle model significantly reduced the cost function in the Southern Ocean for the Southern Hemisphere spring (OND), but increased model-data bias for tropical and the northern regions, so that the overall optimization generated only a slight improvement in the predictions. The consideration of nitrate data from WOA reduced the model-data bias further, especially in the JFM months where the cost function is reduced by 9%. This outcome emphasizes the important role of variation of data sets in parameter optimization experiments. Results from the regional assimilation of SeaWiFS chlorophyll data showed a substantial improvement in the reduction of the model-data misfit in both the northern and southern mid-to-high latitude regions. In some experiments, the inclusion of growth parameters in the assimilation further reduces the model-data misfit.

[32] This study suggests that the adjoint method is applicable to a three-dimensional marine ecosystem model. Several limitations are eminent from the adjoint approach. For example, it is problematic to find a global minimum in a nonlinear complex ecosystem model (for details see auxiliary Text S2). Another example is the sensitivity of inverse approach to the selection of control parameters. Most of the parameters selected in this study are base on a first guess sensitivity test, but future identical twin experiment are necessary to analyze other important in the model such as parameters associated with the air-sea gas exchange,  $N_2$  fixation, iron fertilization, or particle flux parameterization. Moreover, other formulation of the cost function may improve the optimization (e.g., by adding a background term in the cost function).

### 6.2. A Posteriori Model and Observation Evaluation

[33] The following section highlights limitations of the model and the data as identified by significant model-data bias in some regions. In general, the adjoint method is feasible to reduce reasonably the overall model-data misfit, but some of the observed chlorophyll features could not be reproduced by the model. For example, the relatively high a posteriori model-data bias remains in the North Pacific and North Atlantic during the OND and JFM months, and in the Southern Ocean for all months except OND. The simulated chlorophyll concentrations remain relatively low in those regions. The low zooplankton carbon budget from the RAC experiments could imply that the a priori control parameters in the model may overpredict the zooplankton grazing at certain regions of the world ocean. The remaining a posteriori model-data bias can be categorized into uncertainties associated with the physical and biogeochemical parameterizations, and uncertainties associated with the data sampling and sampling strategies.

[34] First, the assimilation in this study assumes that the LSG model is perfect. The German Ocean Model Intercomparison Project (OMIP) and the Ocean Carbon-Cycle Model Intercomparison Project (OCMIP) pointed out some limitations of the current model ([http://www.awi-bremerhaven.de/Modelling/GLOBAL/projects/omip/omip\\_report.pdf](http://www.awi-bremerhaven.de/Modelling/GLOBAL/projects/omip/omip_report.pdf) [*Orr et al.*, 2001]). While the physical model is generally

able to reproduce the observed radiocarbon distribution in the ocean (auxiliary Figure S3), limitation of the prediction may be related to the coarse resolution of the ocean circulation model and the assumptions made in the primitive equations. These uncertainties may be associated with the parameterization of deep water formation and in the diffusion and eddy parameterization, which affect the distribution of the tracers in the ocean and biogeochemical processes.

[35] Second, the model simulation includes uncertainties related to the biogeochemical parameterizations such as parameterization of air-sea carbon fluxes and autotrophic carbon and  $N_2$  fixation process by phytoplankton [Hood *et al.*, 2006]. The fluxes of carbon within the euphotic zone also critically depends on the multi-element growth limitation factor [Aumont *et al.*, 2003], plankton size and community structure [Doney *et al.*, 2003]. Carbon fluxes between the euphotic and deep ocean are sensitive to the remineralization process and the parameterization of vertical POC flux [Howard *et al.*, 2006] as well as the ratio of particle export to primary production [Dunne *et al.*, 2005]. Schlitzer [2000] and Usbeck *et al.* [2003] applied the adjoint method to optimize the export POC flux parameterization. A future challenge would be to test the sensitivity of these parameterizations and calibrate the model with these parameterizations to the observational evidence.

[36] Third, the model-data bias can also be contributed by the data itself. The selection and frequencies of the data sets introduced in the assimilation are very important in the determining optimization performance [Lawson *et al.*, 1996]. The difficulty in replicating the observed chlorophyll in the Southern Ocean may depend on the iron limitation features; thus, the model error may be reduced when additional spatially and temporally resolving iron data is included in the assimilation. Unfortunately, iron observations are still extremely rare and limited. Testing the assimilation using monthly data sets, instead of seasonal, is on the way. Despite the fact that satellite data is advantageous in providing better spatial and temporal coverage than in situ data, significant inconsistencies remains [O'Reilly *et al.*, 2000] and these errors may not necessarily follow a Gaussian distribution.

## 7. Conclusions

[37] The adjoint method was applied to a complex three-dimensional LSG-HAMOCC5.1 to analyze the sensitivity of the model-generated chlorophyll with respect to control parameters and optimize them. Identical twin experiments reveal a substantial reduction of the model-data misfit by the adjoint approach. Many of the sensitive parameters are associated with zooplankton dynamics, such as DOC excretion rate of zooplankton, grazing rate, herbivores egestion rate as fecal pellets, and assimilation efficiency of zooplankton. This implies that zooplankton activities play an important role in the euphotic ecosystem dynamics [LeQuéré *et al.*, 2005]. It also confirms previous study of Smetacek [2001], which showed that the marine phytoplankton dynamics are sensitive to loss (i.e., grazing by zooplankton) processes. Thus future measurements of eco-

system parameters associated with zooplankton dynamics would be crucial for improving the understanding of current ecosystem processes.

[38] When SeaWiFS chlorophyll observation was assimilated into the adjoint model, the model-data misfit was significantly reduced and the a posteriori run still produces realistic carbon flux prediction. The most notable improvement occurs in the high latitude, when the ecosystem parameters are varied for different regions and seasons. The a posteriori model simulation suggested that the model considerably overestimate the NPP in the OND months, but slightly underestimate the NPP in the other months. Future investigations may consider a more detailed analysis of coupled physical biogeochemical system associated with these discrepancies.

[39] **Acknowledgments.** We thank Ernst Maier-Reimer for providing the HAMOCC5 model, valuable discussion, and advice. We acknowledge the SeaWiFS project and the Distributed Active Archive Center at the Goddard Space Flight Center, Greenbelt, Maryland, for the production and distribution of the SeaWiFS data. We thank the anonymous reviewers for their critical and constructive feedbacks. We thank Gijs deBoer, Matt Howard, Valerie Benesh, and Mark Marohl for reading and commenting on the manuscript. This research at the University of Wisconsin Center for Climatic Research is supported by NASA (NAG-11245), the EU North Atlantic Carbon Exchange Study, and the JGOFS (03F0321E) and NSF-EAR (0628336). Center for Climatic Research contribution 878.

## References

- Antoine, D., J.-M. André, and A. Morel (1996), Oceanic primary production: 2. Estimation at global scale from satellite (coastal zone color scanner) chlorophyll, *Global Biogeochem. Cycles*, 10, 57–69.
- Arakawa, A., and V. R. Lamb (1977), Computational design of the basic dynamical processes of the UCLA general circulation model, *Methods Comput. Phys.*, 16, 173–283.
- Aumont, O., E. Maier-Reimer, S. Blain, and P. Monfray (2003), An ecosystem model of the global ocean including Fe, Si, P colimitations, *Global Biogeochem. Cycles*, 17(2), 1060, doi:10.1029/2001GB001745.
- Behrenfeld, M., E. Boss, D. A. Siegel, and D. M. Shea (2005), Carbon-based ocean productivity and phytoplankton physiology from space, *Global Biogeochem. Cycles*, 19, GB1006, doi:10.1029/2004GB002299.
- Berger, W. H. (1989), Global maps of ocean productivity, in *Productivity of the Oceans: Present and Past*, edited by W. H. Berger, V. S. Smetacek, and G. Wefer, pp. 429–455, John Wiley, Hoboken, N. J.
- Chester, R. (2000), Dissolved gasses in sea water, in *Marine Geochemistry*, 2nd ed., pp. 165–199, Blackwell Science, Malden, Mass.
- Doney, S. C., K. Lindsay, and J. K. Moore (2003), Global ocean carbon cycle modeling, in *Ocean Biogeochemistry*, edited by M. J. R. Fasham, pp. 217–238, Springer, New York.
- Dunne, J. P., R. A. Armstrong, A. Gnanadesikan, and J. L. Sarmiento (2005), Empirical and mechanistic models for the particle export ratio, *Global Biogeochem. Cycles*, 19, GB4026, doi:10.1029/2004GB002390.
- Eppley, R. W. (1972), Temperature and phytoplankton growth in the sea, *Fish. Bull.*, 70, 1063–1085.
- Errico, R. M. (1997), What is an adjoint model?, *Bull. Am. Meteorol.*, 2577–2591.
- Evans, G. T. (2003), Defining misfit between biogeochemical models and data sets, *J. Mar. Syst.*, 40/41, 49–54.
- Falkowski, P. G., R. T. Barbere, and V. Smetacek (1998), Biogeochemical controls and feedbacks on ocean primary production, *Science*, 281, 200–206.
- Fennel, K., M. Losch, J. Schröter, and M. Wenzel (2001), Testing a marine ecosystem model: Sensitivity analysis and parameter optimization, *J. Mar. Syst.*, 28, 45–63.
- Friedrichs, M. A. M. (2001), A data assimilative marine ecosystem model of the Central Equatorial Pacific: Numerical twin experiments, *J. Mar. Res.*, 59, 859–894.
- Friedrichs, M. A. M. (2002), Assimilation of JGOFS EqPac and SeaWiFS data into a marine ecosystem model of the central equatorial Pacific Ocean, *Deep Sea Res., Part II*, 49, 289–319.
- Garcia-Goriz, E., N. Hoepffner, and M. Ouberdous (2003), Assimilation of SeaWiFS data in a coupled physical-biological model of the Adriatic Sea, *J. Mar. Syst.*, 40/41, 233–252.

- Gent, P. R., J. Willebrand, T. McDougall, and J. C. McWilliams (1995), Parameterizing eddy-induced tracer transport in the ocean circulation models, *J. Phys. Oceanogr.*, *25*, 463–474.
- Giering, R. (1989), Assimilation von satellitendaten in ein dreidimensionales numerisches model de atlantischen zirkulation, M. S. thesis, Univ. of Hamburg, Hamburg, Germany.
- Giering, R., and T. Kaminski (1998), Recipes for adjoint code construction, *Trans. Math. Software*, *24*, 437–474.
- Gilbert, J. C., and C. Lemaréchal (1989), Some numerical experiments with variable-storage quasi-Newton algorithms, *Math. Program.*, *45*, 407–435.
- Gordon, H. R., and A. Y. Morel (1983), *Remote Assessment of Ocean Color for Interpretation of Satellite Visible Imagery: A Review*, 114 pp., Springer, New York.
- Gregg, W. W., and N. W. Casey (2004), Global and regional evaluation of the SeaWiFS chlorophyll data set, *Remote Sens. Environ.*, *93*, 463–479.
- Hemmings, J. C. P., M. A. Srokosz, P. Challenor, and M. J. R. Fasham (2004), Split-domain calibration of an ecosystem model using satellite ocean colour data, *J. Mar. Syst.*, *50*, 141–179.
- Hofmann, E. E., and M. A. M. Friedrichs (2002), Predictive modeling for marine ecosystems, in *The Sea*, vol. 12, edited by A. J. Robinson et al., pp. 537–565, John Wiley, Hoboken, N. J.
- Hood, R. R., et al. (2006), Pelagic functional group modeling: Progress, challenges and prospects, *Deep Sea Res., Part II*, *53*, 459–512.
- Howard, M. T., A. M. E. Winguth, C. Klaas, and E. Maier-Reimer (2006), Sensitivity of ocean carbon tracer distributions to particulate organic flux parameterizations, *Global Biogeochem. Cycles*, *20*, GB3011, doi:10.1029/2005GB002499.
- Lawson, L. M., E. E. Hofmann, and Y. H. Spitz (1996), Time series sampling and data assimilation in a simple marine ecosystem model, *Deep Sea Res., Part II*, *43*, 625–651.
- Le Quéré, C., et al. (2005), Ecosystem dynamics based on plankton functional types for global ocean biogeochemistry models, *Global Change Biol.*, *11*, 2016–2040, doi:10.1111/j.1365-2486.2005.01004.x.
- Longhurst, A. (1998), *Ecological Geography of the Sea*, Elsevier, New York.
- Losa, S. N., G. A. Kivman, and V. A. Ryabchenko (2004), Weak constraint parameter estimation for a simple ocean ecosystem mode: what can we learn about the model and data?, *J. Mar. Syst.*, *45*, 1–20.
- Maier-Reimer, E. (1993), Geochemical cycles in an ocean general circulation model: Preindustrial tracer distributions, *Global Biogeochem. Cycles*, *7*, 645–677.
- Maier-Reimer, E., and K. Hasselmann (1987), Transport and storage of CO<sub>2</sub> in the ocean—An inorganic ocean-circulation carbon cycle model, *Clim. Dyn.*, *2*, 63–90.
- Maier-Reimer, E., U. Mikolajewicz, and K. Hasselmann (1993), Mean circulation of the Hamburg LSG OGCM and its sensitivity to the thermohaline surface forcing, *J. Phys. Oceanogr.*, *23*, 731–757.
- McClain, C. R., M. L. Cleave, G. C. Feldman, W. W. Gregg, and S. B. Hooker (1998), Science quality of SeaWiFS data for global biosphere research, *Sea Technol.*, *39*(9), 10–17.
- Mikolajewicz, U., M. Groger, E. Maier-Reimer, G. Schurgers, M. Vizcaino, and A. Winguth (2006), Long-term effects of anthropogenic CO<sub>2</sub> emissions simulated with a complex earth system model, *Clim. Dyn.*, in press.
- Natvik, L. J., and G. Evensen (2003), Assimilation of ocean colour data into a biochemical model of the North Atlantic: 1. Data assimilation experiments, *J. Mar. Syst.*, *40/41*, 127–153.
- O'Reilly, J. E., et al. (2000), Ocean color chlorophyll algorithms for SeaWiFS OC2 and OC4: Version4, *SeaWiFS Postlaunch Tech. Rep. Ser. 11*, NASA Goddard Space Flight Center, Greenbelt, Md.
- Orr, J. C., et al. (2001), Estimates of anthropogenic carbon uptake from four three-dimensional global ocean models, *Global Biogeochem. Cycles*, *15*, 43–60.
- Oschlies, A. (2006), On the use of data assimilation in biogeochemical modeling, in *Ocean Weather Forecasting*, edited by E. P. Chassignet, and J. Verron, pp.525–547, Springer, New York.
- Sarmiento, J. L., N. Gruber, M. A. Brzezinski, and J. P. Dunne (2004), High-latitude controls of thermocline nutrients and low latitude biological productivity, *Nature*, *427*, 56–60.
- Schartau, M., A. Oschlies, and J. Willebrand (2001), Parameter estimates of a zero-dimensional ecosystem model applying the adjoint method, *Deep Sea Res., Part II*, *48*, 1769–1800.
- Schlitner, R. (2000), Applying the adjoint method for global biogeochemical modeling, in *Inverse Method in Global Biogeochemical Cycles*, *Geophys. Monogr. Ser.*, vol. 114, edited by P. Kasibhatla et al., pp.107–124, AGU, Washington, D. C.
- Six, K., and E. Maier-Reimer (1996), Effects of plankton dynamics on seasonal carbon fluxes in an ocean general circulation model, *Global Biogeochem. Cycles*, *10*, 559–583.
- Smetacek, V. (2001), A watery arms race, *Nature*, *411*, 745.
- Spitz, Y. H., J. R. Moisan, and M. R. Abbott (2001), Configuring an ecosystem model using data from the Bermuda Atlantic Time Series (BATS), *Deep Sea Res., Part II*, *48*, 1733–1768.
- Talagrand, O. (1991), The use of adjoint equations in numerical modeling of the atmospheric circulation, in *Automatic Differentiation of Algorithms: Theory, Implementation and Application*, edited by A. Griewank, and G. Corliss, pp. 169–180, Soc. of Ind. and Appl. Math., Philadelphia, Pa.
- Thacker, W. C. (1989), The role of the Hessian matrix in fitting models to measurements, *J. Geophys. Res.*, *94*, 6177–6196.
- Tjiputra, J. (2004), Analysis of seasonal chlorophyll and nutrient distribution using an adjoint three-dimensional ocean carbon cycle model, M. S. thesis, 70 pp., Univ. of Wis.-Madison, Madison.
- Usbeck, R., R. Schlitner, G. Fischer, and G. Wefer (2003), Particle fluxes in the ocean: Comparison of sediment trap data with results from inverse modeling, *J. Mar. Syst.*, *39*, 167–183.
- Visbeck, M., J. Marshall, T. Haine, and M. Spall (1997), Specification of eddy transfer coefficients in coarse-resolution ocean circulation models, *J. Phys. Oceanogr.*, *27*, 381–402.

---

D. Polzin, J. F. Tjiputra, and A. M. E. Winguth, Department of Atmospheric Oceanic and Space Sciences, University of Wisconsin-Madison, 1225 West Dayton Street, Madison, WI 53706, USA. (jtjiputra@wisc.edu)